Supplementary Material to

Non-linear frequency-dependent selection promotes long-term coexistence between bacteria species

Noémie Harmand[1], Valentine Federico[1], Thomas Hindré [2], Thomas Lenormand[1 *]

1. UMR 5175 CEFE, CNRS - Université Montpellier - Université P. Valéry - EPHE, Montpellier Cedex 5, France

2. Univ. Grenoble Alpes, Centre National de la Recherche Scientifique (CNRS), Grenoble Institut National Polytechnique (INP), Techniques de l'Ingénierie Médicale et de la Complexité - Informatique, Mathématiques et Applications, Grenoble (TIMC-IMAG), F-38000 Grenoble, France

* corresponding author

Table of contents

1. Common mechanisms of coexistence

Mechanism of coexistence	Example	Reference
(1) Different types specialize on different limiting resources and density is locally regulated	Coexistence of two specialists on two resources as in Levene model	(Levene 1953; Hedrick 1978; Ravigné et al. 2004; Bürger 2010)
(2) Traits or life-stages trade-offs with each other in the exploitation of the same resource	Trade-off between growth rate and conversion efficiency	(Levin 1972; Heino et al. 1997; Bonsall 2006)
(3) A modification of the resource/environment by one type which directly benefits a second type	(a) One type makes the resource more easily accessible as with producer/scrounger strategies (b) One type produces a secondary resource in cross-feeding (c) Other facilitation situations	(a) (Barnard and Sibly 1981) (b) (Helling et al. 1987; Rosenzweig et al. 1994; Treves et al. 1998; Doebeli 2002; Rozen et al. 2009; Plucain et al. 2014; Goldford et al. 2018) (c) (Thijs et al. 1994; Dugatkin et al. 2005; Kelsic et al. 2015))
(4) The behavior of a third party (predator, parasite, mutualist) can specifically benefit rare types	When e.g. rare preys ignored by predator (apostatic selection)	(Clarke 1962; Oaten and Murdoch 1975; Allen 1988; Joron and Mallet 1998; Borghans et al. 2004; Fincke 2004; Olendorf et al. 2006)
(5) Interactions between individuals are more favorable when they involve different types or favor rare types	(a) Interactions between different types such as with mating types, sexes. (b) Interactions favoring rare types such as cheaters in public good games	(a)(e.g. Gross 1996; Sinervo and Lively 1996; Penn and Potts 1999; Reusch et al. 2001) (b) (e.g. O'Connell and Johnston 1998; Gigord et al. 2001; Cordero and Polz 2014)

Table S1. Common mechanisms of coexistence

2. Supplementary methods

Medium and antibiotic

Experimental coevolution and competition assays were performed in Davis minimal medium (DM: 7 g/L $KH_2PO_4.3H_20$, 2 g/L KH_2PO_4, 1 g/L $(NH_4)_2SO_4$, 0.5 g/L $Na_3C_6H_5O_7$, sterile water compensating exactly for evaporation after autoclaving; pH set at 7.0) supplemented with 1250 µL/L glucose 10%, 806 µL/L MgSO4 [1M] and 1000 µL/L thiamine 0.2% (medium referred to as DM250, which supports a stationary-phase cell density of about 5 x 10^8 per mL). Nal was added to the medium at different desired concentrations acting as different abiotic conditions from aliquots at 30 mg/mL diluted in NaOH 300mM. Fresh medium was prepared each week and kept protected from light at 4°C.

Strains

44 *E. coli* evolving lines were initiated from 44 Nal-resistant mutants obtained from the REL4536 clone isolated from the Ara-1 population of the Lenski's LTEE after 10,000 generations of evolution in DM25 (corresponding to DM250 with ten times less glucose) and genetically engineered to constitutively express yellow fluorescent proteins (YFP) (see details in Gallet et al. 2012; Harmand et al. 2017, 2018). Prior to the coevolution, eight lines were allowed to evolve for approximately 400 generations in DM250 at each of five different Nal concentrations (5 x 8 = 40 lines): 3, 8, 20, 100 and 200 µg/mL (these units are not repeated below and referred to as Nal3, Nal8, Nal20, Nal100, Nal200). During this period, the different lines adapted to their dose and were close to their respective optimum (Harmand et al. 2018). Four lines also adapted in the absence of Nal.

C initial strain was obtained from an external contamination (this strain has never been used in our lab) of the glycerol stock that was used for storing the 44 *E* evolution lines. It was identified from the appearance of few non-fluorescent colonies when populations were plated on petri dishes that exhibit a diauxic growth curve in DM250 medium containing both glucose and citrate, the latter not being catabolized by *E. coli* in aerobic conditions. Sequencing and alignment of the 16S ribosomal DNA revealed them as *C. freundii.* No other contaminants were detected. Sequencing of highly variable 16S regions III and VI were performed to control for genetic variability of *C. freundii* among the initial contaminated glycerol stocks. No differences were observed supporting that the contamination occurred only once and with the same *C* strain. This *C* stain is highly Nal resistant, with a MIC in the range Nal600-Nal800.

Experimental coevolution

The 44 coevolutionary replicates (hereafter CRep) with *E* and *C* were cultured (37°C, 250 rpm) from glycerol stocks in 2mL wells of 96-plates containing 1mL DM250 with Nal at different concentrations: 0, 3, 8, 20, 100 and 200 μg/mL (8 CRep in each concentration but 4 at concentration 0). DM250 supports a stationary-phase density of about 5 x 10^8 cells per mL. So the initial -80°C stocks prepared from stationary phase cultures using the contaminated glycerol solution should have contained a large majority of *E* cells (the stocks were prepared by mixing 750uL of stationary phase culture with 250uL of glycerol 60%). CRep were inoculated directly from a preculture inoculated from glycerol stocks into 1ml of DM250. Starting cell densities of the present evolution experiment were about 5 x 10^5 cells per mL. Bacterial populations were propagated for ~870 generations by serial daily transfer using a 1:100 dilution allowing ~6.64 generations per 24h-cycle. Each day, 10μL of cultures in stationary phase were transferred to 990μL of fresh DM250 medium and further incubated at 37°C for 24h. The CRep were stored at regular intervals. The frequencies of *E* and *C* were estimated for each CRep at ca. 0, 200, 550 and 870 generations by counting the number of YFP-fluorescent cells in a sample of 100,000 cells with a flow cytometer (FACSCanto II, BD Biosciences). In five CRep (one at Nal0, two at Nal3, one at Nal100 and one at Nal200), more than 98% cells were typed as YFP throughout the experiment. It is difficult to exclude from cytometry data that *C* was present at very low frequencies in these replicates, as a few non-fluorescent *C* cells cannot be easily distinguished from background noise. As a second check, some plating done on these five CRep did not reveal the presence of *C*. Hence, the absence of *C* in these replicates presumably reflect that *C* did not establish from the start in these cases. On the contrary, low frequencies of *E* are more easily detected as these cells carry YFP fluorescence allowing easy discrimination from background noise.

Strains isolation

E and *C* were isolated based on phenotypic differences between the two species: *C* can grow on citrate only, whereas *E* cannot, and *E* is resistant to streptomycin (Str), while *C* is not. CRep were grown for 24h at 37°C both in DM-Nal without glucose and in DM250-Nal-Str. The cultures were then diluted and plated on LB plates in order to obtain isolated colonies after overnight growth at 37°C. We checked that colonies from the culture in DM250-Nal-Str were all fluorescent, contrary to the colonies from the DM-Nal cultures. Each time, cells from six different colonies of both *E* and *C* type were collected from DM250-Nal-Str and DM-Nal cultures respectively, mixed, and stored for further experiments. Hence, *E* and *C* samples isolated at each time point do not represent a single clone, and are referred to as 'lines'.

Characterization

We measured growth curves of isolated *E*0, *C*0, *E*2, *C*2, and *E*8, *C*8 lines from CRep20A and CRep20B. The cultures were made as in the conditions of the experimental evolution (DM250-Nal20, start at 1:100 volumic ratio). Optical density was recorded during a 24h growth cycle at 37°C.

In order to test whether the strong curvature of the NFDS pattern at low frequency of *E* could result from an unknown cross-feeding (i.e. whether *E* could consume a metabolite produced and not consumed by *C*, we measured growth of *E* lines isolated from CRep20A and CRep20B in a filtrate of the growth medium of the *C* lines. Growth curves were measured as described above.

To investigate the effect of the citrate dose on growth patterns, we measured growth curves of 12 *E* and 12 *C* isolated lines at six different citrate concentrations (ranging from 0 to 2 times the concentration) in DM250-Nal20. Growth curves were measured as described above. We used *E* and *C* lines isolated from one CRep in each Nal dose of coevolution, at the initial and final time of the coevolution.

Fitness measures

E and *C* lines were first cultured separately overnight in DM250-Nal20 in the same conditions as the experimental evolution. The cultures were then mixed in 1mL wells with 21-22 different volumic frequencies from 0.01% to 99% of *E* . 10 μL of those mixes were transferred to 1 mL of DM250-Nal20 and allowed to compete for 24h at 37°C, 250 rpm. Each competition was done in duplicate except for time-shifted competitions. Frequencies of *E* and *C* cells at time 0 and 24h were estimated using a flow cytometer (FACSCanto II, BD Biosciences), counting 100,000 cells. Selection coefficients per generation were calculated in a standard way, as in Harmand *et al.* (2018), eq. (1).

3. Resource-based models for modelling negative frequency dependent selection

The following model is inspired by Manhart et al. (2018), adding diauxic growth on two resources. The model overview is illustrated on Fig. S1. We considered a case where two bacterial strains (*E* and *C*) are in competition in a medium containing two resources. The strain *E* consumes only one resource (denoted R_1) and the strain *C* consumes first the resource R_1 and then switches toward the other resource (denoted R_2). The competition lasts until both resources have been depleted. The consumption of a resource results in three phases for the population dynamics: a lag phase, an exponential phase and a stationary phase when the resource is exhausted. The population size changes only during the exponential phase. The expressions for the growth functions of *E* and *C* across those phases are thus:

$$N_E(t) = \begin{cases} x\,N(0), & 0 \le t \le \lambda_E \\ x\,N(0)\,e^{r_E\,(t-\lambda_E)}, & \lambda_E < t < t_{switch} + \Delta t \\ x\,N(0)\,e^{r_E\,(t_{sat1}+\Delta t-\lambda_E)}, & t \ge t_{switch} + \Delta t \end{cases} \quad (1)$$

For *E* and

$$N_C(t) = \begin{cases} (1-x)\,N(0), & 0 \le t \le \lambda_{C1} \\ (1-x)\;N(0)\,e^{r_{C1}\,(t-\lambda_{C1})}, & \lambda_{C1} < t < t_{switch} \\ (1-x)\;N(0)\,e^{r_{C1}\,(t_{switch}-\lambda_{C1})}, & t_{switch} \le t \le t_{switch} + \lambda_{C2} \\ (1-x)\,N(0)\,e^{r_{C1}\,(t_{switch}-\lambda_{C1})+\,r_{C2}\,(t-t_{switch}-\lambda_{C2})}, & t_{switch} + \lambda_{C2} < t < t_{switch} + t_{sat2} \\ (1-x)\,N(0)\,e^{r_{C1}\,(t_{switch}-\lambda_{C1})+\,r_{C2}\,(t_{sat2}-\lambda_{C2})}, & t \ge t_{switch} + t_{sat2} \end{cases} \quad (2)$$

for *C*. The notations in these equations are given in Table S2. The amount of resource 1 consumed at the time when *C* switches to resource 2 ($R_1 - R_{1switch}$) can be expressed from the cell numbers at this time and the efficiency parameters as:

$$R_1 - R_{1switch} = \frac{N_E\,(t_{switch})}{Y_E} + \frac{N_C\,(t_{switch})}{Y_{C1}}$$

$$R_{1switch} = \frac{N_E\,(t_{switch}+\Delta t) - N_E\,(t_{switch})}{Y_E} \quad (3)$$

$$R_2 = \frac{N_C\,(t_{switch} + t_{sat,C2})}{Y_{C2}}$$

The selection coefficient of *E* against *C* is defined as:

$$s = \mathrm{Log}\left(\frac{N_E(t_{switch} + \Delta t)}{N_C(t_{switch} + t_{sat2})}\right) - \mathrm{Log}\left(\frac{N_E(0)}{N_C(0)}\right) = r_{\mathrm{E}}\,(t_{switch} + \Delta t - \lambda_{\mathrm{E}}) + r_{\mathrm{C1}}\,(\lambda_{\mathrm{C1}} - t_{switch}) + r_{\mathrm{C2}}\,(\lambda_{\mathrm{C2}} - t_{sat2}) \quad (4)$$

This equation is used to introduce *s* in the expressions for $R_{1switch}$ and $R_1 - R_{1switch}$ in (3). This is done by replacing the term $r_E\,(t_{switch} - \lambda_E)$ by $s + r_{\mathrm{C1}}\,(t_{switch} - \lambda_{\mathrm{C1}}) + r_{\mathrm{C2}}(t_{sat2} - \lambda_{\mathrm{C2}}) - r_E\,\Delta t$. The system (3) is then solved for t_{switch}, Δt and t_{sat2} and the resulting expressions are replaced in the expression of *s* in (4). This equation is finally solved numerically in Mathematica 9, to obtain *s* values corresponding to different parameter values. Figure 6 illustrates the NFDS patterns expected under the three different mechanisms.

First (Fig. 6a), we investigated the case where two types can coexist when exploiting the same resource. This can occur when one type is specialized on growth rate while the other one is specialized on conversion efficiency. The 'efficient converter' can be favored when rare, possibly leading to NFDS with an internal equilibrium, provided the conversion advantage is large. This is illustrated in Fig. 6a with increased conversion efficiency for one type compared to a baseline. This mechanism is not very likely in our case, as it requires very large differences in conversion efficiency, which are not noticeable on the individual growth curves. It also does not reproduce the shape of the observed NFDS patterns well, and does not account for diauxic growth in *C*.

Second (Fig. 6b), we investigated cases involving competition on two resources. We consider a baseline situation (black line) *E* and *C* are equally able to exploit resource 1 (glucose), but *C* can also exploit resource 2 (citrate). In this baseline situation, *C* is favored at all frequencies, and especially when rare due to this private niche on citrate, as observed in our results. NFDS can only emerge if *E* is better at exploiting resource 1 (with a shorter lag phase or equivalently a higher growth), as represented by the lighter grey curves (the larger the advantage of *E* on resource 1, the lighter the curve). This situation is similar to a Levene model with *E* as a better competitor on

glucose, and *C* as a better competitor on citrate. However, in this simple model, contrary to our observations, there is no strong non-linearity of the NFDS pattern when *E* is rare.

Third (Fig. 6c), we investigated the same case as above, except that *C* switches to citrate before glucose is depleted (i.e. when the quantity of glucose equals $R_{1switch}$, which is below R_1). This might occur if there is a selection pressure on *C* to switch to citrate earlier and if the metabolic activity on glucose is, as is likely, reduced after the onset of this switch. The selection pressure for an early switch may be caused by competition for citrate within *C* alone, independently of the presence of *E*. With such an early switch, the glucose niche is divided into two sub-niches: one where *C* and *E* are competing and one that can be privately exploited by *E*. This last sub-niche corresponds to the amount of glucose left at the time of *C*'s citrate-switch ($R_1 - R_{1switch}$). This switch could be triggered in response to a reduced concentration of glucose (Wang et al. 2015). Note that this switch does not require that *C* consumption rate of glucose drops instantaneously to zero. A model where this drop is more gradual or where *C* still consumes glucose at a small rate after the time of switch (smaller than that of *E*), would give qualitatively similar results. Fig. 6c illustrates the shapes of the NFDS pattern that emerge when this glucose private niche becomes larger (i.e. when $R_{1switch}$ is smaller so that the diauxic switch occurs earlier for *C*). These "S-shaped" patterns are generally consistent with the NFDS patterns we observe (Fig. 3).

The model can be used to determine ways to mimic the variation of the NFDS patterns seen in the data. Fig. 3d provides an example of time variation fitted to match CRep20A is presented, but the situation is closely similar for CRep20B. *E* parameters are kept constant, and only *C* evolves. Initially (at time T0) *E* has an advantage on glucose (either in terms of growth rate, lag, or conversion efficiency). *C* can consume both glucose and citrate, but switches to citrate before glucose is depleted (which creates the *S*-shaped NDFS pattern signature). At generation 200 (T2), the NDFS pattern shifts down but mostly at high frequency (step1 arrow). This can be obtained by increasing *C* conversion efficiency on citrate, but with an earlier *C* switch to citrate (leaving more 'private' glucose to *E*). At final time (T8), the NDSFS pattern shifts down mostly at low frequency (step2 arrow). This can be obtained if *C* keeps its conversion efficiency on citrate but evolves back to a later switch to citrate (i.e. leaving less 'private' glucose to *E* compared to T2). Note that other *C* parameters can evolve without altering the NDFS pattern against *E*. For instance, growth rate and lag on citrate can evolve (as seen in Fig. 4), as a result of within-*C* competition, but this is not changing the fitness relative to *E* (as *E* does not consume citrate). Finally, the effect of Nal concentration on equilibrium frequency of *E* and *C* can be easily obtained by assuming that the growth (reduced growth rate or increased lag) of *E* on glucose is reduced with increasing Nal concentration (i.e. that this reduction is greater for *E* than *C*, even though both are resistant and survive at the different Nal concentrations), as shown on Fig 3e.

Parameters	$\boldsymbol{x}$	E initial frequency
	λ_E , λ_{C1} , λ_{C2}	Lag time of E on glucose, of C on glucose, of C on citrate, respectively
	r_E , r_{C1} , r_{C2}	Growth rate of E on glucose, of C on glucose, of C on citrate, respectively
	Y_E , Y_{C1} , Y_{C2}	Conversion efficiency of E on glucose, of C on glucose, of C on citrate, respectively
	R_1, R_2	Quantities of glucose and citrate
	$R_{1switch}$	Quantity of glucose triggering metabolic switch of C from glucose to citrate
Variables	$N(t)$, $N_E(t)$, $N_C(t)$	total cell number at time t, E cell number at time t, C cell number at time t
	t_{sat2}	Time of resource 2 depletion
	$t_{switch} + \Delta t$	Time of resource 1 depletion
	t_{switch}	Time of metabolic switch of C from glucose to citrate

Table S2. Summary of model notations

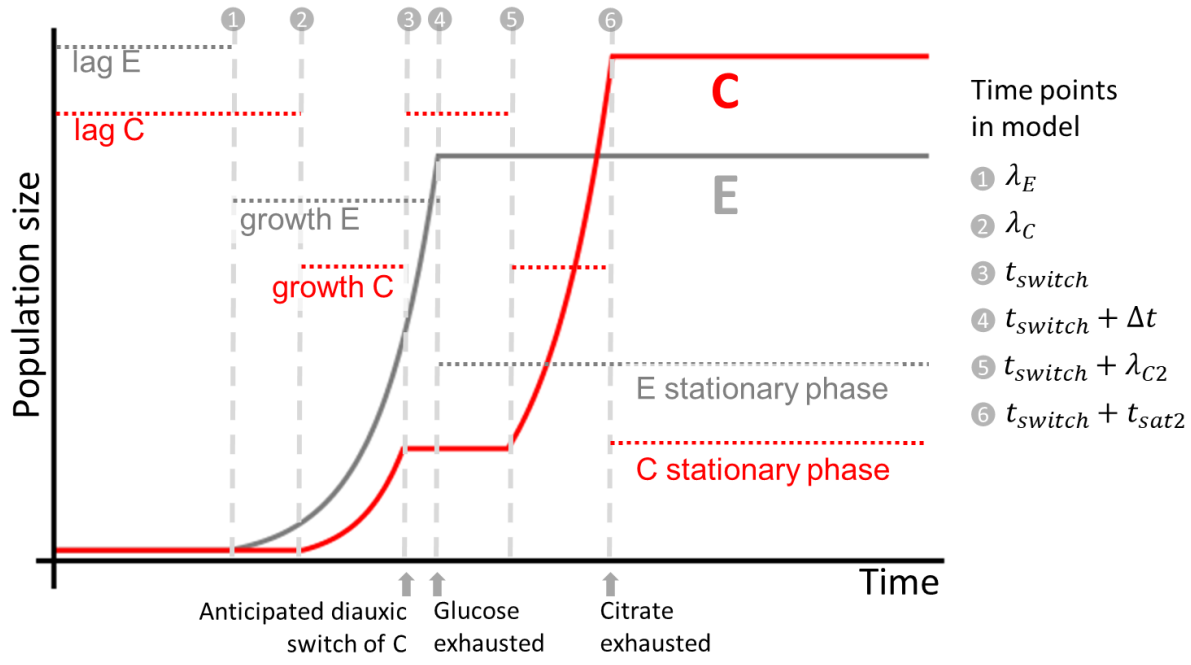

Figure S1. Illustration of the growth curves of each species considered in the model.

4. Growth patterns at different citrate concentration

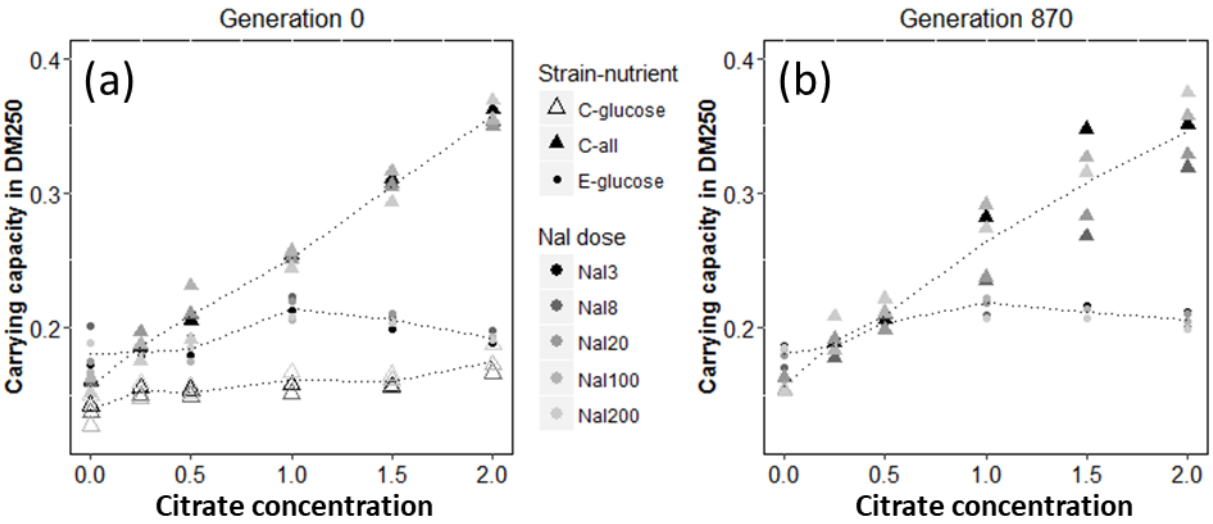

Figure S2. Effect of citrate concentration (normalized such that 1 corresponds to the concentration used for experimental evolution) on growth in DM250-Nal20 of *E. coli* (dots) and *C. freundii* (triangles) lines in DM250 at different Nal doses initially (panel a) or at the end of the coevolution (panel b). The average optical density is used as a measure of the carrying capacity of each line in the medium. For *E*, there is a single plateau, and the maximal averaged optical density during the stationary phase indicates the carrying capacity (*E*-glucose). For *C*, there is a diauxic growth curve: the maximal averaged optical densities at the first and second plateau are carrying capacities indicated by open (*C*-glucose) and filled triangles (*C*-all), respectively. At the final time point of the coevolution (panel b), the first plateau was no longer identifiable due to a very short lag time for citrate consumption, so carrying capacity is computed from the maximal optical density at the second plateau only (*C*-all).

5. Growth patterns in filtrated medium

E did not grow in the filtrated medium produced after a growth cycle of *C* as shown on Figure S3. Hence the strong curvature of the NFDS pattern at low frequency of *E* cannot be explained by cross-feeding through a metabolite produced and left unconsumed by *C*.

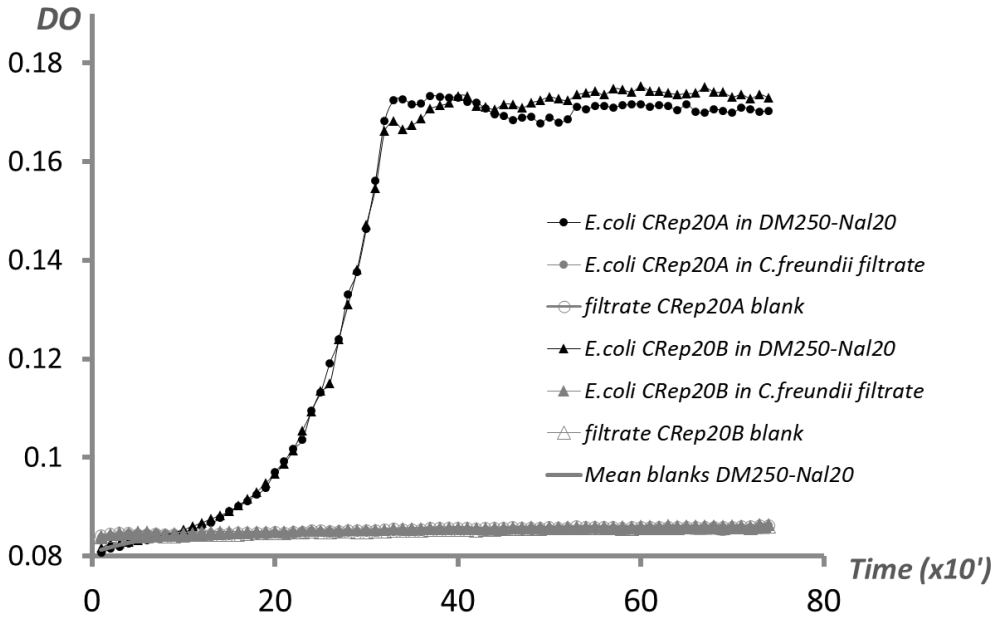

Figure S3. Growth curve of *E.coli* CRep20A and CRep20B on filtrated medium obtained after a growth cycle of *C. freundii* CRep20A and CRep20B in DM250-Nal 20 at generation 0. *x*-axis: time in 10mins units; *y*-axis: optical density.

References

Allen, J. A. 1988. Frequency-dependent selection by predators. Philos. Trans. R. Soc. Lond. B. Biol. Sci. 319:485–503.

Barnard, C. J., and R. M. Sibly. 1981. Producers and scroungers: A general model and its application to captive flocks of house sparrows. Anim. Behav. 29:543–550.

Bonsall, M. B. 2006. Longevity and ageing: appraising the evolutionary consequences of growing old. Philos. Trans. R. Soc. Lond. B. Biol. Sci. 361:119–135.

Borghans, J. A. M., J. B. Beltman, and R. J. De Boer. 2004. MHC polymorphism under host-pathogen coevolution. Immunogenetics 55:732–739.

Bürger, R. 2010. Evolution and polymorphism in the multilocus Levene model with no or weak epistasis. Theor. Popul. Biol. 78:123–138.

Clarke, B. 1962. Balanced polymorphism and the diversity of sympatric species. Pp. 47–70 *in* D. Nichols, ed. Taxonomy and Geography. Systematics Association, Oxford.

Cordero, O. X., and M. F. Polz. 2014. Explaining microbial genomic diversity in light of evolutionary ecology. Nat Rev Microbiol 12:263–273.

Doebeli, M. 2002. A model for the evolutionary dynamics of cross-feeding polymorphisms in microorganisms. Popul Ecol 44:59–70.

Dugatkin, L. A., M. Perlin, J. S. Lucas, and R. Atlas. 2005. Group-beneficial traits, frequency-dependent selection and genotypic diversity: an antibiotic resistance paradigm. Proc. Biol. Sci. 272:79–83.

Fincke, O. M. 2004. Polymorphic signals of harassed female odonates and the males that learn them support a novel frequency-dependent model. Anim. Behav. 67:833–845.

Gallet, R., T. F. Cooper, S. F. Elena, and T. Lenormand. 2012. Measuring selection coefficients below 10 -3: Method, Questions, and Prospects. Genetics 190:175–86.

Gigord, L. D., M. R. Macnair, and A. Smithson. 2001. Negative frequency-dependent selection maintains a dramatic flower color polymorphism in the rewardless orchid *Dactylorhiza sambucina* (L.) Soo. Proc. Natl. Acad. Sci. U. S. A. 98:6253–6255.

Goldford, J. E., N. Lu, D. Bajić, S. Estrela, M. Tikhonov, A. Sanchez-Gorostiaga, D. Segrè, P. Mehta, and A. Sanchez. 2018. Emergent simplicity in microbial community assembly. Science 361:469–474.

Gross, M. R. 1996. Alternative reproductive strategies and tactics: diversity within sexes. Trends Ecol. Evol. 11:92–98.

Harmand, N., R. Gallet, R. Jabbour-Zahab, G. Martin, and T. Lenormand. 2017. Fisher's geometrical model and the mutational patterns of antibiotic resistance across dose gradients. Evolution 71:23–37.

Harmand, N., R. Gallet, G. Martin, and T. Lenormand. 2018. Evolution of bacteria specialization along an antibiotic dose gradient. Evol. Lett. 2:221–232.

Hedrick, P. W. 1978. Genetic variation in a heterogeneous environment. V. Spatial heterogeneity

in finite populations. Genetics 89:389–401.

Heino, M., J. A. J. Metz, and V. Kaitala. 1997. Evolution of mixed maturation strategies in semelparous life histories: the crucial role of dimensionality of feedback environment. Philos. Trans. R. Soc. B Biol. Sci. 352:1647–1655.

Helling, R., C. Vargas, and J. Adams. 1987. Evolution of *Escherichia coli* during growth in a constant environment. Genetics 116:349–358.

Joron, M., and J. L. B. Mallet. 1998. Diversity in mimicry: Paradox or paradigm? Trends Ecol. Evol. 13:461–466.

Kelsic, E. D., J. Zhao, K. Vetsigian, and R. Kishony. 2015. Counteraction of antibiotic production and degradation stabilizes microbial communities. Nature 521:516–519.

Levene, H. 1953. Genetic equilibrium when more than one ecological niche is available. Am. Nat. 87:331–333.

Levin, B. 1972. Coexistence of Two Asexual Strains on a Single Resource. Science 175:1272–1274.

Manhart, M., B. V. Adkar, and E. I. Shakhnovich. 2018. Trade-offs between microbial growth phases lead to frequency-dependent and non-transitive selection. Proc. R. Soc. B Biol. Sci. 285:20172459.

O'Connell, L. M., and M. O. Johnston. 1998. Male and Female Pollination Success in a Deceptive Orchid, a Selection Study. Ecology 79:1246–1260.

Oaten, A., and W. W. Murdoch. 1975. Functional response and stability in predator-prey systems. Am. Nat. 109:289–298.

Olendorf, R., F. H. Rodd, D. Punzalan, A. E. Houde, C. Hurt, D. N. Reznick, and K. a Hughes. 2006. Frequency-dependent survival in natural guppy populations. Nature 441:633–636.

Penn, D. J., and W. K. Potts. 1999. The evolution of mating preferences and major histocompatibility complex genes. Evolution 153:145–164.

Plucain, J., T. Hindré, M. Le Gac, O. Tenaillon, S. Cruveiller, C. Médigue, N. Leiby, W. R. Harcombe, C. J. Marx, R. E. Lenski, and D. Schneider. 2014. Epistasis and allele specificity in the emergence of a stable polymorphism in *Escherichia coli*. Science 343:1366–1369.

Ravigné, V., I. Olivieri, and U. Dieckmann. 2004. Implications of habitat choice for protected

polymorphisms. Evol. Ecol. Res. 6:125–145.

Reusch, T. B. H., M. A. Häberli, P. B. Aeschlimann, and M. Milinski. 2001. Female sticklebacks count alleles in a strategy of sexual selection explaining MHC polymorphism. Nature 414:300–302.

Rosenzweig, R. F., R. R. Sharp, D. S. Treves, and J. Adams. 1994. Microbial evolution in a simple unstructured environment: Genetic differentiation in *Escherichia coli*. Genetics 137:903–917.

Rozen, D. E., N. Philippe, J. Arjan de Visser, R. E. Lenski, and D. Schneider. 2009. Death and cannibalism in a seasonal environment facilitate bacterial coexistence. Ecol. Lett. 12:34–44.

Sinervo, B., and C. M. Lively. 1996. The rock-paper-scissors game and the evolution of alternative male strategies. Nature 380:240–243.

Thijs, H., J. R. Shann, and J. D. Weidenhamer. 1994. The effect of phytotoxins on competitive outcome in a model system. Ecology 75:1959–1964.

Treves, D. S., S. Manning, and J. Adams. 1998. Repeated evolution of an acetate-crossfeeding polymorphism in long-term populations of *Escherichia coli*. Mol. Biol. Evol. 15:789–97.

Wang, J., E. Atolia, B. Hua, Y. Savir, R. Escalante-Chong, and M. Springer. 2015. Natural variation in preparation for nutrient depletion reveals a cost-benefit tradeoff. PLoS Biol. 13:1–31.